Supplemental Information

GluD2- and Cbln1-mediated Competitive Interactions Shape the Dendritic Arbors of Cerebellar Purkinje Cells

Yukari H. Takeo, S. Andrew Shuster, Linnie Jiang, Miley Hu, David J. Luginbuhl, Thomas Rülicke, Ximena Contreras, Simon Hippenmeyer, Mark J. Wagner, Surya Ganguli, Liqun Luo

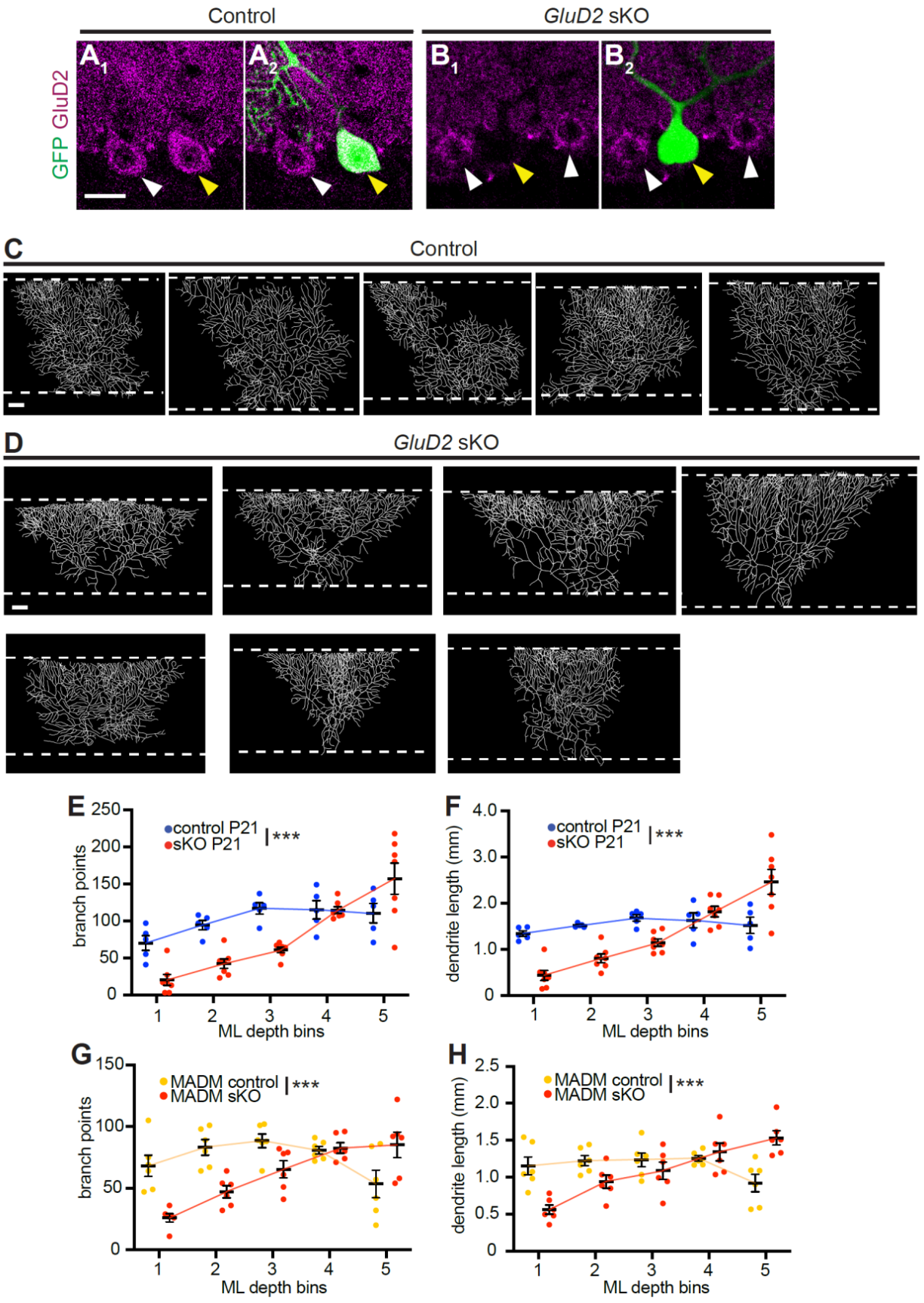

Figure S1. Morphological Characteristics of *GluD2* sKO Purkinje Cells, Related to Figure 1

(A, B) GluD2 staining (magenta) in representative P21 control (A) and *GluD2* sKO (B) Purkinje cells generated via *in utero* electroporation (labeled by GFP, green) and neighboring cells. Yellow arrowheads indicate normal GluD2 staining in a control cell (A_1) and a lack of GluD2 staining in a *GluD2* sKO cell (B_1). White arrowheads indicate unlabeled neighboring cells.
(C, D) Dendritic tracings of control (C) and *GluD2* sKO (D) Purkinje cell dendrites. Scale bars, 20 μm.
(E–H) Distribution of the number of dendritic branch points (E, G) and dendrite length (F, H) in each molecular layer (ML) depth bin in P21 control (blue) and *GluD2* sKO (red) (E,F), or P21 MADM control (yellow) and MADM *GluD2* sKO (red) (G, H, see also **Figure S2A-E**) cells. The normalized data as a ratio to the total number of branch points or total dendrite length is shown in **Figure 1E, F, K, L**. Data are mean ± SEM; n = 5 control, 7 sKO cells from 2 (control), 3 (sKO) mice for E, F; n = 6 $GluD2^{+/-}$ MADM control, 6 $GluD2^{-/-}$ MADM sKO cells from 2 mice for K, L; ***$p < 0.001$; two-way ANOVA.

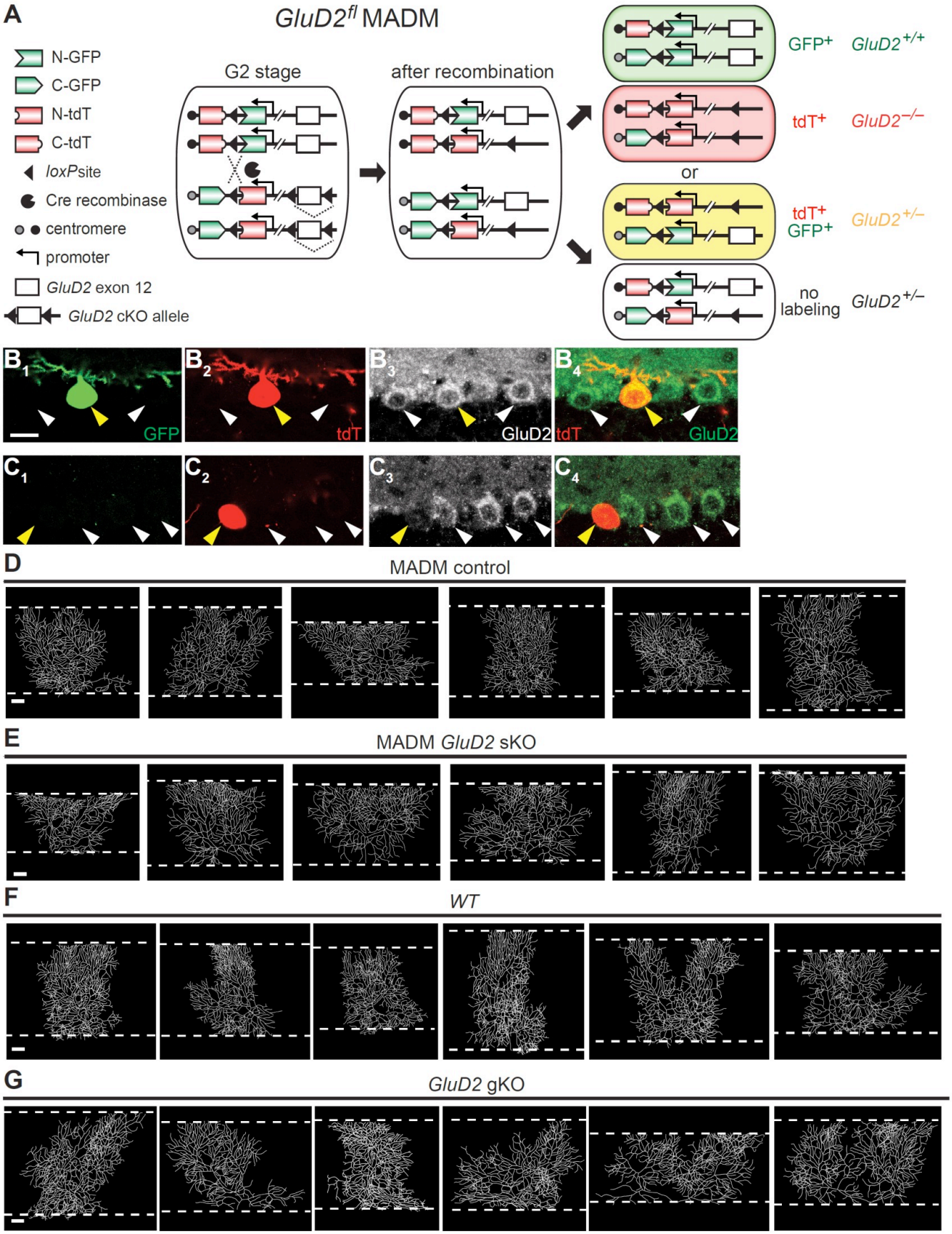

Figure S2. Morphological Characteristics of MADM *GluD2* sKO and Global *GluD2* Knockout Purkinje Cells, Related to Figures 1 and 3

(A) MADM schematic illustrating inter-chromosomal recombination leading to sparsely-labeled *GluD2*$^{+/+}$, *GluD2*$^{+/-}$, and *GluD2*$^{-/-}$ (*GluD2* sKO) cells. See Contreras et al. (2020) for detail.
(B, C) GluD2 staining in representative MADM-labeled GFP^{+}/tdT^{+} *GluD2*$^{+/-}$ control (B) and GFP^{-}/tdT^{+} *GluD2*$^{-/-}$ sKO (C) cells, as well as neighboring *GluD2*$^{+/-}$ cells not labeled by MADM. Yellow arrowheads indicate normal GluD2 staining in a MADM control cell (B_3) and a lack of GluD2 staining in a MADM *GluD2* sKO cell (C_3). White arrowheads indicate unlabeled neighboring cells.
(D, E) Tracings of MADM control (*GluD2*$^{+/-}$, D) and GluD2 sKO (*GluD2*$^{-/-}$, E) Purkinje cell dendrites.
(F, G) Tracings of control (*wild-type*, F) and *GluD2* global knockout (gKO, G) Purkinje cell dendrites, related to Figure 3.
Scale bars, 20 μm.

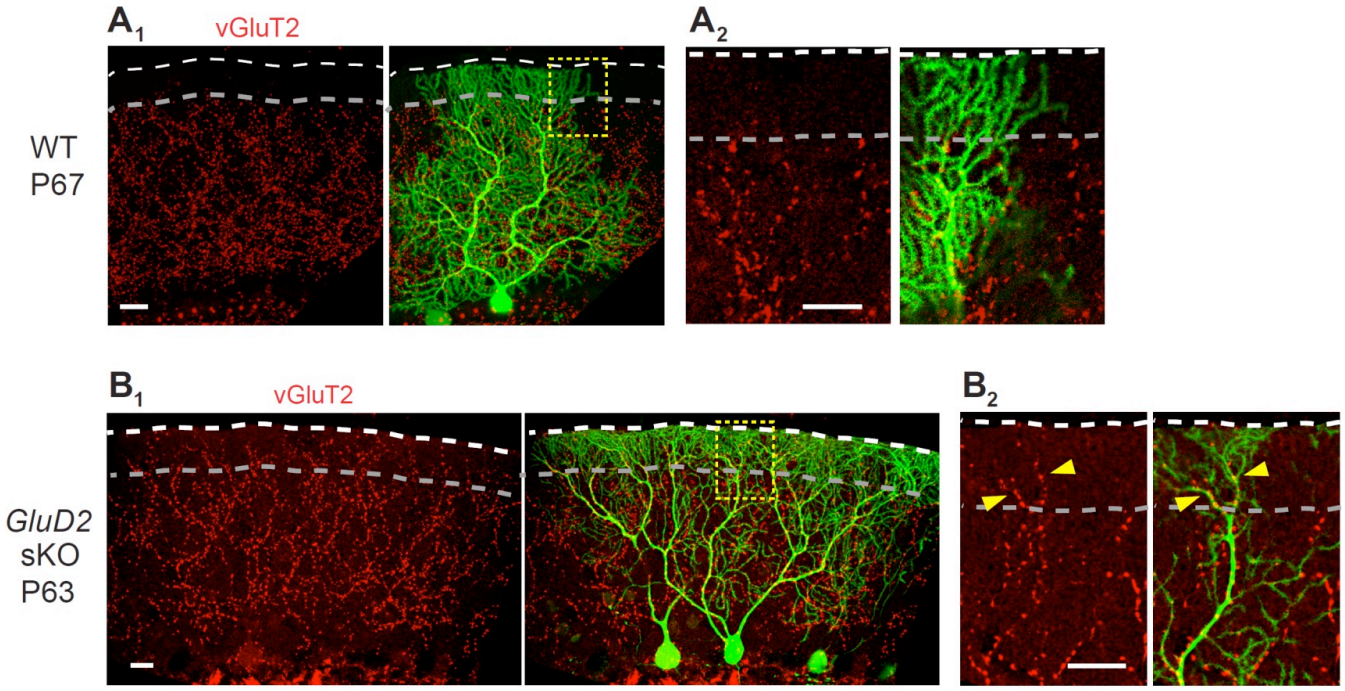

Figure S3. *GluD2* sKO Disrupts Climbing Fiber Innervation, Related to Figure 2.
Representative confocal images of vGluT2 staining (red) of tdTomato-electroporated *wild-type* (WT) P67 (A) or GFP-electroporated *GluD2* sKO P63 (B) Purkinje cells. Green indicates tdTomato or GFP to label the Purkinje cell dendritic trees. A_1 and B_1 are the low magnification z-stacked images. A_2 and B_2 are the single-section high magnification images of the boxed regions of A_1 and B_1. The white dashed lines indicate the pial surface. The gray dashed lines represent the top 20% superficial molecular layer at which vGluT2 staining is normally absent in wild-type conditions. Arrowheads show expansion of vGluT2 puncta to the superficial molecular layer apposed to GFP^+ *GluD2* sKO cells. Scale bars, 20 µm.

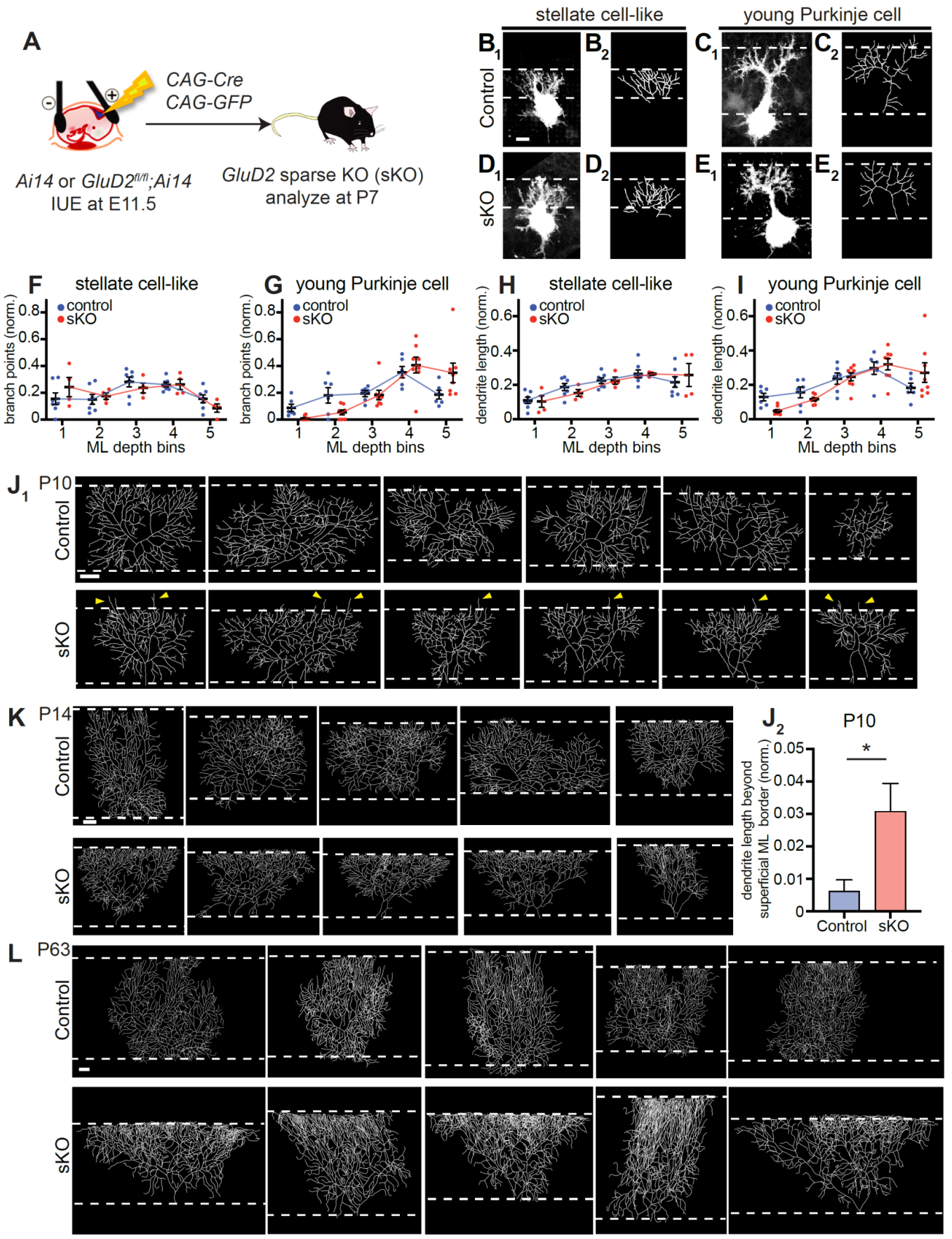

Figure S4. Additional Data on Developmental Analysis of *GluD2* sKO, Related to Figure 4

(A) Schematic of *in utero* electroporation (IUE) for genetically accessing Purkinje cells in control *Ai14* and *GluD2*$^{fl/fl}$*;Ai14* embryos. Plasmids encoding Cre recombinase and GFP were co-injected into the fourth ventricle at embryonic day 11.5 (E11.5). Cerebellar samples were collected at postnatal day 7 (P7).
(B–E) Representative confocal images (B_1–E_1) and tracings (B_2–E_2) of control (B, C) and *GluD2* sKO (D, E) Purkinje cells at P7. These trees were categorized as stellate cell-like (with 3+ primary dendrites) or young Purkinje cells (with 1–2 primary dendrites). Scale bar, 10 μm.
(F–I) Quantification of the normalized number of branch points (F, G) and dendrite length (H, I) in each molecular layer (ML) depth bin in control (blue) and *GluD2* sKO (red) Purkinje cells in the stellate cell-like (F, H) and young Purkinje cell categories (G, I). Data was normalized to the total number of dendritic branch points or dendrite length across the tree. While control and sKO stellate-like cells appear similar at P7, in the young Purkinje cell category, there is a trend toward sKO cells having fewer dendritic branch points and reduced proximal dendrite length in bin 1 and more dendritic branch points and increased distal dendrite length in bin 5.
(J–L) Dendritic tree tracings of P10 (J_1), P14 (K), and P63 (L) control and *GluD2* sKO cells. J_2, Quantification of normalized dendrite length that extends beyond the superficial border of the molecular layer. Data are mean ± SEM; n = 6 (control), 6 (sKO) cells from 2 animals each; *$p < 0.05$; t test.
Scale bars, 20 μm.

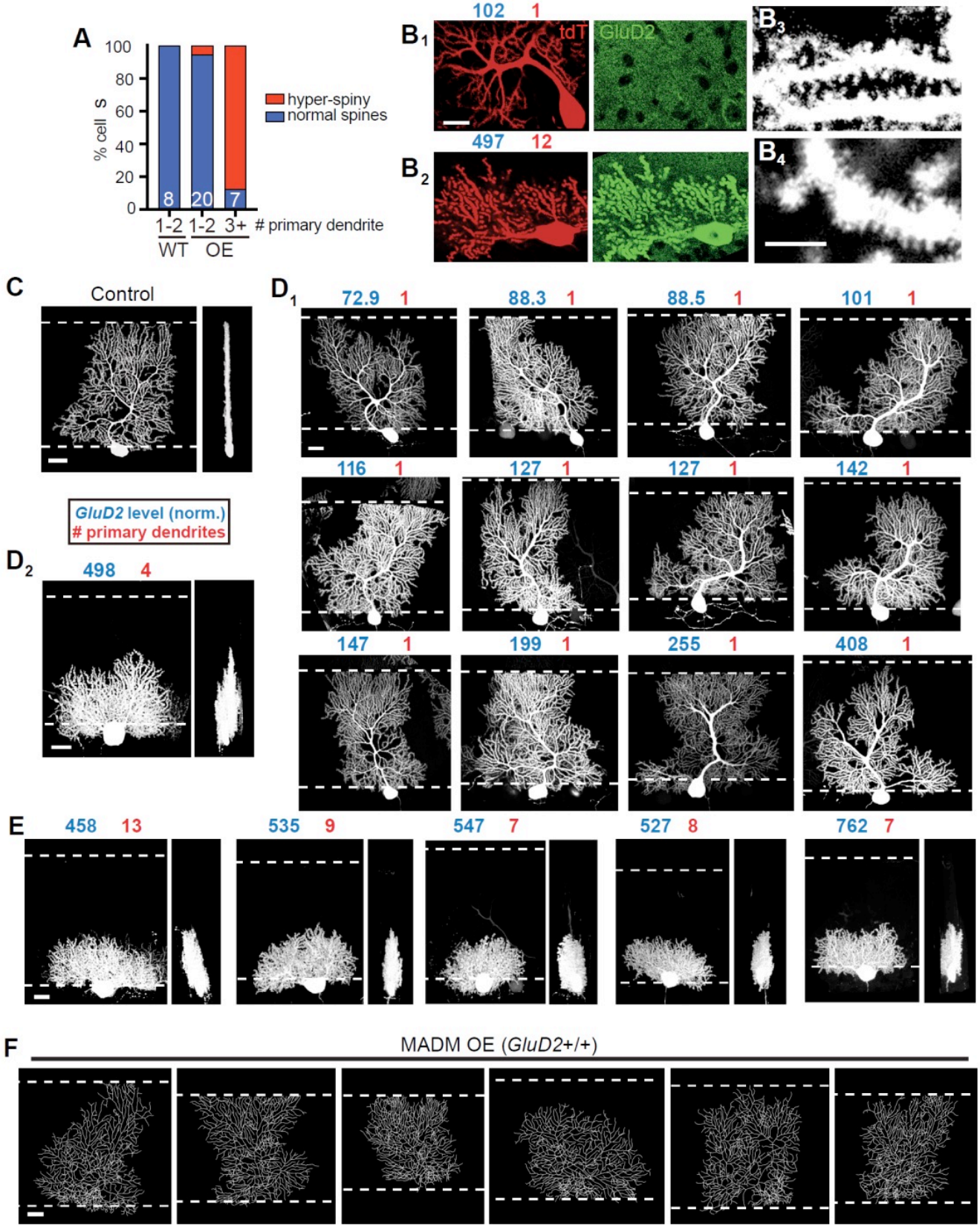

Figure S5. Morphological Characteristics of GluD2 OE Purkinje Cells, related to Figure 5
(A) Percentage of hyper-spiny and normal cells according to genotype and number of primary dendrites. The numbers of cells within each category are indicated.

(B) Representative images of GluD2 staining (B_1, B_2) and dendritic spines (B_3, B_4) of GluD2 OE Purkinje cells used for quantifications shown in Figure panels 5D, G, H, and S5A. GluD2 intensity (relative to control) and number of primary dendrites are indicated in blue and red numbers, respectively.
(C) Left, representative z-stack confocal image of a control Purkinje cell at P21. Right, 90-degree rotation of the image, revealing the cell's planarity.
(D) Z-stack confocal images of GluD2 OE Purkinje cells collected in an unbiased manner. Cells were categorized post hoc based on whether they have 1–2 (D_1) or 3+ (D_2) primary dendrites. (D_2) Left, z-stack confocal image of a GluD2 OE Purkinje cell with 4 primary dendrites. Right, 90-degree rotation of the image, revealing a substantially thicker dendritic tree.
(E) Unbiased imaging of entire dendritic trees tended to exclude Purkinje cells with short dendritic trees (e.g., D_2) due to their increased dendritic thickness, which was often cut through in the tissue sections. Therefore, we selected additional GluD2 OE Purkinje cells from new animals, based on their short dendritic trees. Post hoc measurements indicated high GluD2 overexpression levels (blue numbers) and supernumerary primary dendrites (red numbers). Right, images after 90-degree rotations revealing increased dendritic tree thicknesses.
(F) Dendritic tree tracings of MADM *GluD2*$^{+/+}$ cells.
Scale bars: 20 μm (B_1, B_2, C–E); 5 μm (B_3, B_4).

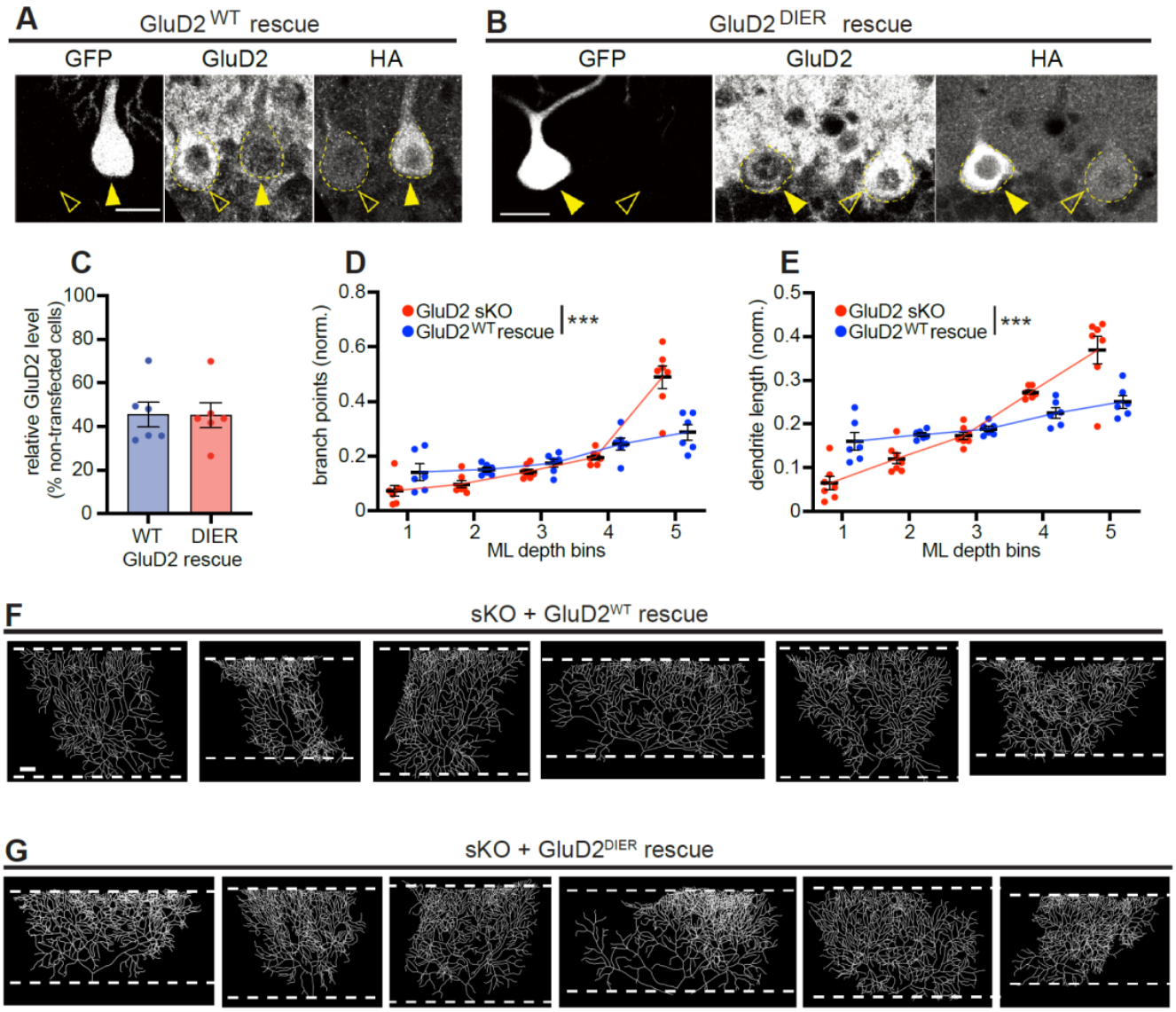

Figure S6. Additional Data on the GluD2 Rescue Experiments, Related to Figure 6

(A, B) Representative images showing GluD2 level in *GluD2*^{WT} rescue (A) and *GluD2*^{DIER} rescue (B) cells. Filled arrowheads indicate cells electroporated with *GluD2* and *GFP* transgenes (as indicated by both HA and GFP staining). Open arrowheads indicate neighboring unlabeled *wild-type* cells.

(C) Quantification of GluD2 staining levels in GluD2^{WT} rescue (A) and GluD2^{DIER} rescue (B) cells.

(D, E) Quantification of the normalized number of branch points (D) and dendrite length (E) in each molecular layer (ML) bin of *GluD2* sKO (red) and GluD2^{WT} rescue (blue) Purkinje cells. Data are mean ± SEM; n = 7 (*GluD2* sKO), 6 (GluD2^{WT} rescue) cells from 3 (*GluD2* sKO), 2 (GluD2^{WT} rescue) mice; ***p < 0.001; two-way ANOVA.

(F, G) Dendritic tree tracings of GluD2^{WT} rescue (D) and GluD2^{DIER} rescue (E) cells.

Scale bars, 20 μm.

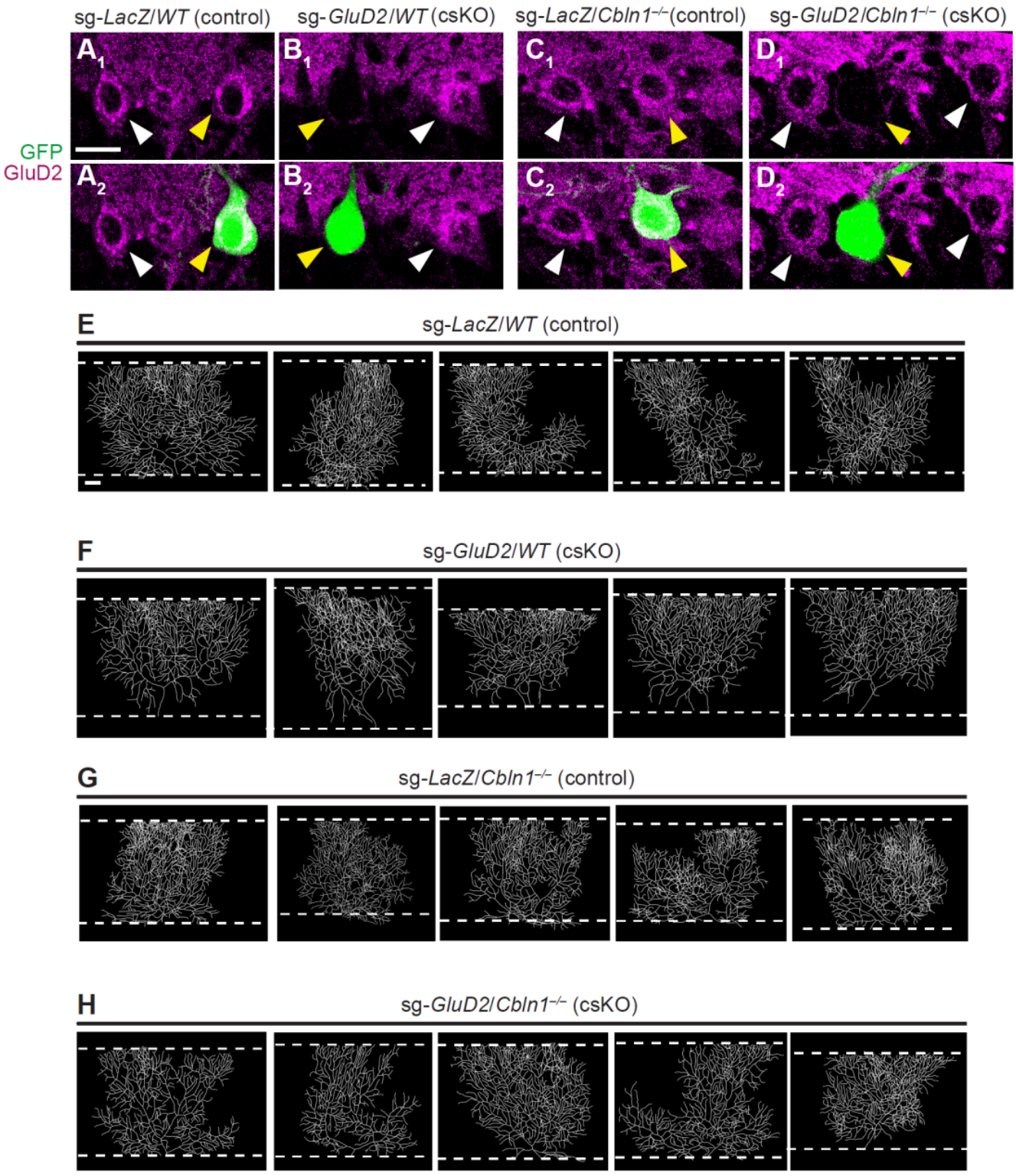

Figure S7. Additional Data on CRISPR-mediated *GluD2* sKO in *Wild-type* and *Cbln1*$^{-/-}$Backgrounds, Related to Figure 7

(A–D) GluD2 staining of Purkinje cells electroporated with sg-*LacZ* (A, C) and sg-*GluD2* (B, D) in *wild-type* (A, B) and *Cbln1*$^{-/-}$ (C, D) backgrounds. Yellow arrowheads indicate GFP^{+} labeled cells showing a lack of GluD2 staining in sg-*GluD2* but not sg-*LacZ* conditions, when compared to neighboring non-labeled cells indicated by white arrowheads.
(E–H) Dendritic tree tracings of sg-*LacZ WT* (E) and *Cbln1*$^{-/-}$ (F) cells and sg-*GluD2 WT* (G) and *Cbln1*$^{-/-}$ (H) cells.
Scale bars, 20 μm.

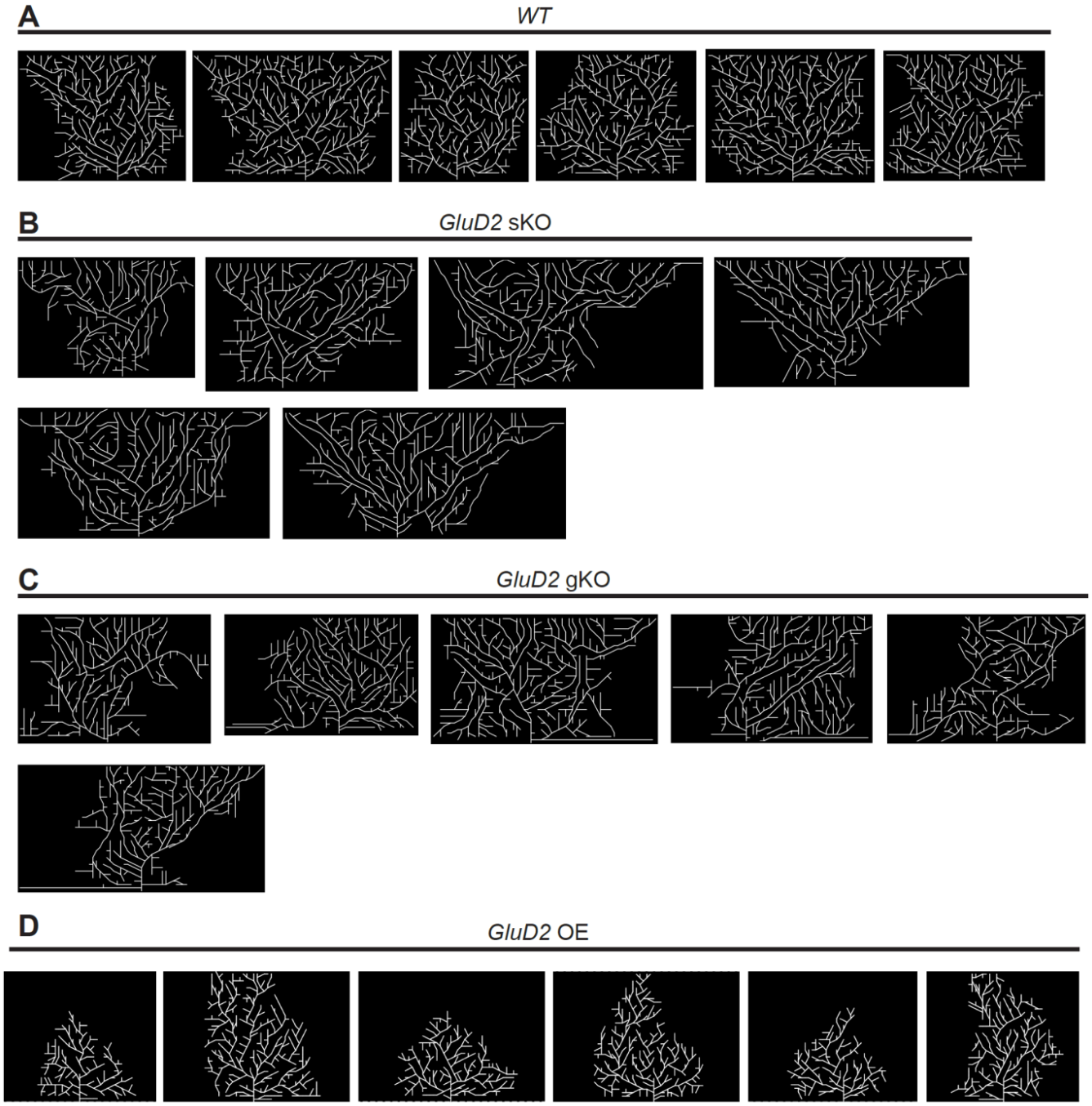

Figure S8. Full Set of Simulation Results, Related to Figure 8
(A) Full set of simulations with three *wild-type* Purkinje cells, showing the middle *wild-type* (*WT*) cell only.
(B) Full set of simulations with one *GluD2* knockout Purkinje cell and two neighboring *wild-type* cells on either side, showing the middle cell only. This mimics the sparse knockout (sKO) experimental condition.
(C) Full set of simulations with *GluD2* knockout Purkinje cells, showing the middle cell only. This mimics the global knockout (gKO) experimental condition.
(D) Full set of simulations with one *GluD2* overexpression Purkinje cell and two neighboring *wild-type* cells on either side, showing the middle cell only. This mimics the sparse overexpression (OE) experimental condition.

Movie S1

Click here to access/download

Supplemental Videos and Spreadsheets

MovieS1.mp4

Movie S2

Click here to access/download

Supplemental Videos and Spreadsheets

MovieS2.mp4

Movie S3

Click here to access/download

Supplemental Videos and Spreadsheets

MovieS3.mp4